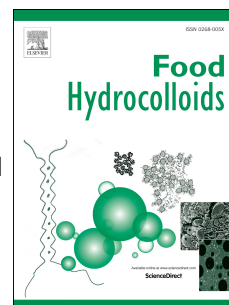


# Accepted Manuscript

Self-association of bovine  $\beta$ -casein as influenced by calcium chloride, buffer type and temperature

Meng Li, Mark A.E. Auty, Shane V. Crowley, Alan L. Kelly, James A. O'Mahony, André Brodkorb



PII: S0268-005X(18)30988-3

DOI: [10.1016/j.foodhyd.2018.09.035](https://doi.org/10.1016/j.foodhyd.2018.09.035)

Reference: FOOHYD 4673

To appear in: *Food Hydrocolloids*

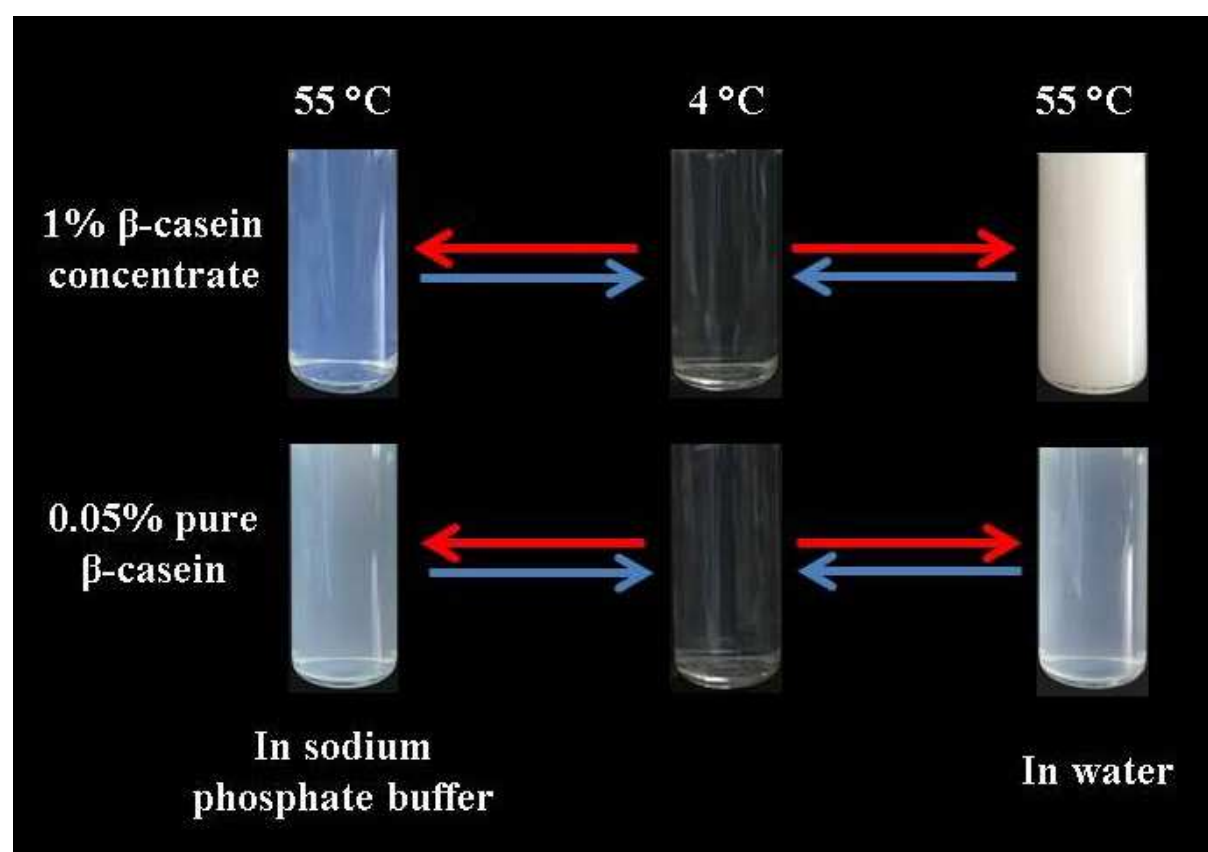
Received Date: 1 June 2018

Revised Date: 21 August 2018

Accepted Date: 24 September 2018

Please cite this article as: Li, M., Auty, M.A.E., Crowley, S.V., Kelly, A.L., O'Mahony, J.A., Brodkorb, André., Self-association of bovine  $\beta$ -casein as influenced by calcium chloride, buffer type and temperature, *Food Hydrocolloids* (2018), doi: <https://doi.org/10.1016/j.foodhyd.2018.09.035>.

This is a PDF file of an unedited manuscript that has been accepted for publication. As a service to our customers we are providing this early version of the manuscript. The manuscript will undergo copyediting, typesetting, and review of the resulting proof before it is published in its final form. Please note that during the production process errors may be discovered which could affect the content, and all legal disclaimers that apply to the journal pertain.



Self-association of bovine  $\beta$ -casein as influenced by calcium chloride, buffer type and temperature

Meng Li<sup>1,2</sup>, Mark A.E. Auty<sup>1</sup>, Shane V. Crowley<sup>2</sup>, Alan L. Kelly<sup>2</sup>, James A. O'Mahony<sup>2</sup>, André Brodkorb<sup>1\*</sup>

<sup>1</sup>*Teagasc Food Research Centre, Moorepark, Fermoy, Co. Cork, Ireland*

<sup>2</sup>*School of Food and Nutritional Sciences, University College Cork, Cork, Ireland*

\*Corresponding author.

Tel.: +353 25 42431

E-mail address: andre.brodkorb@teagasc.ie

## Abstract

The aim of this study was to investigate the aggregation behaviour of a pure  $\beta$ -casein ( $\beta$ -CN<sub>pure</sub>) and a  $\beta$ -casein concentrate ( $\beta$ -CN<sub>conc</sub>) as a function of temperature, presence of  $\text{CaCl}_2$  and buffer type (pH 6.8). The particle size distribution and turbidity of  $\beta$ -casein ( $\beta$ -CN) solutions were measured by dynamic light-scattering (DLS) and UV/vis spectroscopy between 4 and 55 °C. Upon heating (4 to 55 °C), the particle size of both  $\beta$ -CN solutions increased, indicating self-association *via* hydrophobic interactions. It was shown that the self-association of  $\beta$ -CN increased with increasing  $\beta$ -CN concentration and that  $\beta$ -CN<sub>pure</sub> self-associated at significantly lower concentration than  $\beta$ -CN<sub>conc</sub>. Both turbidity and particle size measurements showed that  $\beta$ -CN had similar aggregation behaviour in water and imidazole buffer (pH 6.8) but differed in sodium phosphate buffer (pH 6.8), especially at higher ionic calcium concentrations. In addition, Fourier Transform Infrared (FTIR) spectroscopy revealed very little change in the secondary structure of  $\beta$ -CN during heating (4 to 55°C). The microstructure of  $\beta$ -CN aggregates was monitored during heating from 10 to 55 °C, followed by cooling to 10 °C, using polarised light microscopy. Spherical and heterogeneous aggregates were observed when heated at temperatures above 37 °C, which were reversible upon cooling. This study confirmed that  $\beta$ -CN undergoes self-associates on heating that reverses upon cooling, with the aggregation process being highly dependent on the purity of  $\beta$ -CN, the solvent type and the presence of ionic calcium.

## Keywords:

$\beta$ -casein; Dairy proteins; Protein aggregation.

## 1. Introduction

Caseins and whey proteins are the major proteins in mammalian milk. Bovine milk protein comprises ~80% casein and ~20% whey proteins, whereas the protein in human milk contains ~40% casein and ~60% whey proteins. Caseins consist of four different casein molecules:  $\alpha_{s1}$ -,  $\alpha_{s2}$ -,  $\beta$ - and  $\kappa$ -casein in the ratio 4:1:4:1 (Fox & McSweeney, 2003). In human milk,  $\beta$ -casein ( $\beta$ -CN) constitutes 65% of total casein, which is almost twice that of bovine milk (McSweeney, O'Regan, & O'Callaghan, 2013).  $\beta$ -CN is the major calcium-binding protein in human milk and can efficiently transport inorganic calcium and phosphate to the neonate (Farrell Jr., 1999). Furthermore, it has been reported that  $\beta$ -CN is a precursor for the production of bioactive peptides that have antihypertensive, opioid, or mineral-binding properties (Meisel, 1997). Therefore,  $\beta$ -CN-enriched ingredients are much sought after in the formulation of infant nutritional formulae. However, infant formulae enriched with  $\beta$ -CN may have different physical and functional properties such as heat stability, viscosity, emulsification, digestion etc. These properties are strongly affected by formulation (e.g., protein profile, protein content, mineral content) and processing parameters.

The  $\beta$ -CN molecule is a single polypeptide chain consisting of 209 amino acids with a molecular weight of 24 kDa.  $\beta$ -CN is rich in proline and devoid of cysteine residues, hence there are no intramolecular disulphide bonds.  $\beta$ -casein is an amphiphilic phosphoprotein with a highly hydrophobic region at the C-terminus and a highly hydrophilic negatively-charged region towards the N-terminus (Rollema, 1992), making it an excellent emulsifier (Dickinson, Rolfe, & Dalgleish, 1988; Parkinson & Dickinson, 2004). In bovine  $\beta$ -CN, five phosphate groups are present as esters of the amino acid serine, with the phosphoserine residues located within the hydrophilic domain (Darewicz, Dziuba, Caessens, & Gruppen, 2000; Huppertz et al., 2006); whereas human  $\beta$ -CN occurs in multiphosphorylated forms having 0-5 phosphate groups (Greenberg, Groves, & Dower, 1984). The secondary structure of  $\beta$ -casein has been studied, although the exact structure remains elusive. For decades,  $\beta$ -casein was assumed to have a random coil structure, with little or no ordered secondary structure under physiological conditions (Andrews et al., 1979; Noelken & Reibstein, 1968). Holt and Sawyer (1993) put forward the 'rheomorphic' hypothesis, which states that casein has no fixed structure until aggregates are formed in response to calcium-binding by serine phosphate groups.

Some convincing evidence has been presented to suggest that there are reasonable amounts of fixed structure in  $\beta$ -casein, such as  $\alpha$ -helices,  $\beta$ -turns and  $\beta$ -sheets, probably due to the high proportion of proline residues (Farrell Jr., Wickham, Unruh, Qi, & Hoagland, 2001; Qi, Wickham, & Farrell, 2004). In aqueous solution,  $\beta$ -casein exists as monomers or aggregates, the size and morphology of which are strongly dependent on protein concentration, temperature, calcium content, pH and ionic strength (Dauphas et al., 2005; Moitzi, Portnaya, Glatter, Ramon, & Danino, 2008; O'Connell, Grinberg, & de Kruif, 2003). The critical micellisation concentration (CMC) is defined as the concentration of  $\beta$ -CN above which small aggregates will form. The CMC can vary between 0.05 and 0.2% (w/v) depending on temperature, pH and ionic strength (Portnaya et al., 2006). Monomers of  $\beta$ -CN predominate at low temperatures ( $< 10$ - $15\text{ }^{\circ}\text{C}$ ) and self-assemble *via* hydrophobic interactions above the CMC when temperature increases, thereby forming aggregates with a hydrophobic core and a less dense hydrophilic outer layer (Dauphas et al., 2005; O'Connell et al., 2003). This temperature-dependent property has been used for the purification of  $\beta$ -CN from  $\beta$ -CN-enriched whey through membrane filtration (Atamer et al., 2017; O'Mahony, Smith, & Lucey, 2014).

Dauphas et al. (2005) suggested there were four different aggregation states of  $\beta$ -CN (0.1%, w/v) based on DLS experiments; a molecular state at  $4\text{ }^{\circ}\text{C}$  (7-8 nm), a micellar state at  $37\text{ }^{\circ}\text{C}$  (20-25 nm) in the absence of calcium chloride, and a polymeric state at  $4\text{ }^{\circ}\text{C}$  (20-25 nm) and an aggregated state at  $37\text{ }^{\circ}\text{C}$  ( $> 1\text{ }\mu\text{m}$ ) in the presence of calcium chloride (10 mM). Adding calcium or increasing ionic strength can lead to an increase in aggregate size due to the reduction of electrostatic repulsions, which can lead to precipitation/sedimentation under certain conditions (Dickinson, 2001). In addition, the self-association of  $\beta$ -CN is affected by various dispersant constituents, such as urea, Tris-HCl buffer, sodium phosphate buffer and ethanol (Mikheeva, Grinberg, Grinberg, Khokhlov, & de Kruif, 2003; Qi et al., 2004). Micellisation of  $\beta$ -CN is a reversible equilibrium process (Dauphas et al., 2005). Increasing temperature changes the equilibrium towards the micelle, by increasing the monomer density in the micelles, whereas increasing ionic strength shifts the equilibrium position, with only a slight effect on the number of monomers in the micelle (Huppertz, 2013).

Over the past two decades, the self-association of  $\beta$ -CN has been studied using a range of analytical approaches, including static and dynamic light-scattering (Dauphas et al., 2005; de Kruif & Grinberg,

2002; Ossowski et al., 2012; Panouillé, Durand, & Nicolai, 2005), small-angle X-ray scattering (Kajiwara et al., 1988; Moitzi et al., 2008), and high-sensitivity differential scanning calorimetry (Mikheeva et al., 2003). The association and dissociation behaviour of  $\beta$ -casein concentrate ( $\beta$ -CNconc) produced by membrane filtration, was previously determined using dynamic light-scattering, analytical centrifugation and turbidimetry by Crowley (2016). DLS is the most widely used technique for measuring particle size distribution. Automated temperature trend DLS allows the measurement to be carried out continuously with a temperature ramp at constant heating rate.

The self-association of  $\beta$ -CN and the stability of  $\beta$ -CN aggregates are mainly attributed to a delicate balance of hydrophobic and electrostatic interactions (Evans, Phillips, & Jones, 1979; Horne, 1998). However, this relationship has not yet been fully understood in the presence of calcium and phosphate. Therefore, a good understanding of the influence of inherent and added salts (calcium and phosphate) on the self-association of  $\beta$ -CN is essential and important for fundamental research but also for the development of  $\beta$ -CN-enriched dairy products.

The main objectives of this research were (1) to study the self-association of  $\beta$ -CN under various experimental conditions, in particular: (a) the effect of the purity (protein profile and mineral content) of  $\beta$ -CN on its self-association behaviour; (b) the effect of selected composition and environmental conditions (temperature, buffer type, calcium addition) on aggregation of  $\beta$ -CN as determined by particle size and turbidity; and (2) to visualise the microstructure and thermo-reversibility of  $\beta$ -CN aggregates in select samples using optical microscopy with a temperature-controlled sample stage.

## 2. Materials and methods

### 2.1. Materials

$\beta$ -CN from bovine milk (spec sheet: 85 % protein,  $\geq 98\%$  purity, lots SLBS9719 and SLBK9882V) and  $\text{CaCl}_2 \cdot 2\text{H}_2\text{O}$  were purchased from Sigma-Aldrich (St. Louis, MO, USA). In addition, a  $\beta$ -CN concentrate powder (87.1% protein, 80%  $\beta$ -CN purity) was kindly donated by the Center for Dairy Research at the University of Wisconsin-Madison, USA. This spray-dried  $\beta$ -CN concentrate was produced at pilot plant scale using an integrated membrane filtration process based on the method of O'Mahony et al. (2014), with some modifications. The protein and mineral profiles for both protein products are presented in Table 1. To differentiate the samples, the pure  $\beta$ -CN (90% purity) from Sigma-Aldrich is referred to as  $\beta$ -CN<sub>pure</sub>, whereas the membrane filtration derived  $\beta$ -CN concentrate (80% purity) is referred to as  $\beta$ -CN<sub>conc</sub>.

Both  $\beta$ -CN powders were dissolved, with agitation, in 10 mM sodium phosphate buffer or 10 mM imidazole-HCl buffer, pH 6.8 at different concentrations of  $\beta$ -CN (0.05%, 0.25%, 0.5% and 1% w/v) for a minimum of 20 h at 4 °C. Distilled water ( $\text{H}_2\text{O}$ ) was used as control. Samples were incubated at temperatures of 4, 37 and 55 °C for 1 h in order to visually observe their thermal aggregation.  $\beta$ -CN concentrations of 0.05% and 1% were finally selected for  $\beta$ -CN<sub>pure</sub> and  $\beta$ -CN<sub>conc</sub>, respectively, for further analysis. The effect of  $\text{CaCl}_2$  (0 and 2.5 mM) addition on  $\beta$ -CN aggregation was also examined. The pH of all samples was adjusted to  $6.8 \pm 0.02$  with a small amount of 1M HCl or 1M NaOH, after which they were filtered at 4 °C through syringe filters of pore size 0.45  $\mu\text{m}$ , to remove large protein aggregates before measurement. The aggregation behaviour of  $\beta$ -CN was studied at a range of temperatures from 4 to 55 °C, and samples were incubated at each temperature for 20 min, unless otherwise indicated. All other reagents were purchased from Sigma-Aldrich, unless otherwise specified.

### 2.2. SDS-polyacrylamide gel electrophoresis (SDS-PAGE)

Protein profile of two  $\beta$ -CN products was determined as described by Yong and Foegeding (2008) using precast NuPAGE 12% Bis-Tris gels (1.0 mm  $\times$  10 well) (Novex<sup>®</sup> by Life Technologies<sup>™</sup>, Carlsbad, CA, USA). Samples were dissolved in NuPAGE LDS sample buffer with NuPAGE sample



reducing agent to achieve a final protein concentration of 0.5 mg/ml, and 10 µl of the mixture was loaded in each well. Skim milk was used as standard. Gels were stained and destained using the method described by Li, Auty, O'Mahony, Kelly, and Brodkorb (2016).

### 2.3. Reversed-phase high pressure liquid chromatography (RP-HPLC)

Characterisation of  $\beta$ -CN samples were also carried out by RP-HPLC (Agilent 1200 series, Agilent Technologies, Santa Clara, CA, USA) as described by McCarthy, Kelly, O'Mahony, and Fenelon (2013) with an Agilent 300 SB-C18 Poroshell column (Agilent Technologies) at 35 °C.  $\beta$ -CN samples were prepared by dilution in 7 M urea/20 mM bis-tris propane buffer, pH 7.5 to obtain a final protein concentration of 2 mg/ml. The sample buffer had  $\beta$ -mercaptoethanol (5 µl/ml buffer) added immediately prior to use. Running buffer A contained 10% acetonitrile and 0.1% trifluoroacetic acid (TFA) in Milli-Q® water. Running buffer B contained 90% acetonitrile, 10% Milli-Q® water, and 0.09% TFA. The analysis was performed using a linear gradient of Buffer B, from 26 to 100% in 26 min. Individual proteins were calculated as percentage (w/w) of total protein by integrating the peak area of the chromatograms.

### 2.4. Turbidity measurement

The turbidity of  $\beta$ -casein solutions reconstituted in three different buffers, with and without  $\text{CaCl}_2$ , was expressed as the optical density (OD) at 600 nm using a Cary 100 Bio UV-visible Spectrophotometer (Varian Inc., Palo Alto, California, USA), which was equipped with a temperature control system. Samples were held at 4 °C before transfer to the spectrophotometer and heated in the chamber at 13 temperature points between 4 and 55 °C. Measurements were taken in triplicate and this experiment was repeated three times.

### 2.5. Dynamic light-scattering (DLS)

The effect of temperature on particle size of  $\beta$ -CN solutions was recorded by DLS using a Zetasizer Nano ZS (Malvern Instruments Ltd, Malvern, Worcestershire, UK), equipped with a temperature controlled cell holder. The instrument was flushed with dry air for measurement below 12 °C to avoid

condensation, according to the instructions by Malvern. Samples were held at 4 °C and further filtered through a 0.22 µm filter before transfer to the thermo-equilibrated zetasizer. Temperature was increased stepwise from 4 to 55 °C with a temperature interval of 3 °C and an equilibration time of 20 min. Measurements were taken six times at each temperature. Data collection and analyses were performed using the Nano software (version 7.01; Malvern Instruments), with a water RI value of 1.33. The temperature-dependence of the solvent viscosity was taken into account for the size calculations.

## 2.6. Fourier Transform Infrared Spectroscopy (FTIR)

FTIR measurements were carried out using a Bruker Tensor 27 instrument (Bruker Optik, GmbH, Germany), equipped with a thermally controlled BioATR II cell. Spectra were obtained using an average of 128 sample scans and 128 background scans at 4 cm<sup>-1</sup> resolution. Samples were filtered through 0.22 µm syringe filters before each measurement at 4, 16, 25, 37, 49 and 55 °C, using fresh dispersions at each temperature. Background readings were taken against distilled water at each measurement temperature. Data analysis was performed as previously described (Kehoe, Remondetto, Subirade, Morris, & Brodkorb, 2008).

## 2.7. Microstructure of β-CN aggregates

The microstructure of β-CN aggregates was assessed using an Olympus BX51 light microscope fitted with differential interference contrast (DIC) filters (Olympus Optical Co. Ltd., Tokyo, Japan). β-CN solution (10 µl) was deposited on a microscopy slide after which a coverslip was placed on the sample, before observation with a 60X, 1.4NA oil immersion objective. The sample slide was placed on a temperature controlled microscope stage, which was controlled by Linksys 32 Software (PE94, Linkam Scientific, UK). Observations were performed during heating (10-55°C), holding for at least 20 min and cooling (55-10 °C) cycles (heating and cooling rates were 3-6°C /min) to evaluate reversibility of β-CN aggregation. Images were acquired using a ProgRes<sup>®</sup> camera system (JENOPTIK I Optical Systems, Jena, Germany) in a DIC mode. The DIC mode highlights phase

boundaries of normally transparent objects and facilitates visualization of the shape and dimension of  $\beta$ -CN aggregates.

## 2.8. Statistical analysis

The preparation of solutions and subsequent analyses were carried out in independent triplicate trials. One-way analysis of variance (ANOVA), followed by Fisher's test, was carried out using the Minitab 15 (Minitab Ltd, Coventry, UK, 2007) statistical analysis package. Differences were stated significant at  $p$ -value  $< 0.05$ .

### 3. Results and discussions

#### 3.1. Compositional properties of $\beta$ -CN products

The protein profile and mineral composition of both  $\beta$ -CN samples were analysed using RP-HPLC and ICP-MS, respectively, and the results are shown in Table 1. It is worth noting that the mineral levels in  $\beta$ -CN<sub>pure</sub> were substantially lower than those of  $\beta$ -CN<sub>conc</sub>, with the exception of sodium. Most notably, Ca content was approximately two orders of magnitude higher in  $\beta$ -CN<sub>conc</sub> compared to that in  $\beta$ -CN<sub>pure</sub>. RP-HPLC profile of  $\beta$ -CN samples are shown in Figure 1A and B, respectively. It was calculated that  $\beta$ -CN<sub>pure</sub> contained 90%  $\beta$ -CN and 5.5%  $\kappa$ -CN, and trace levels of  $\alpha$ -CN and  $\beta$ -lactoglobulin. In contrast,  $\beta$ -CN<sub>conc</sub> has 80%  $\beta$ -CN and 3.9% other caseins and 16% whey proteins, which is consistent with the results of Crowley (2016). The presence of whey proteins may affect the association behaviour of the  $\beta$ -CN during heating. Reducing SDS-PAGE result (Fig. 1C) showed well-resolved band patterns of  $\beta$ -CNs and other proteins (lane 2 and 3). Moreover, a small amount of high molecular weight (MW) whey proteins (possibly lactoferrin and bovine serum albumin) were detected in  $\beta$ -CN<sub>conc</sub> sample (lane 3) by SDS-PAGE.

#### 3.2. Effect of purity and concentration on the thermal aggregation of $\beta$ -CN

The visual appearance of solutions at four  $\beta$ -CN concentrations (0.05, 0.25, 0.5 and 1% w/v), prepared with  $\beta$ -CN<sub>pure</sub> or  $\beta$ -CN<sub>conc</sub> in 10 mM sodium phosphate buffer (pH 6.8) and at 4, 37 and 55 °C are presented in Figure 2. It was observed that the turbidity of  $\beta$ -CN<sub>pure</sub> solutions increased with the temperature, indicating self-association upon heating above 37 °C. In addition, the turbidity of  $\beta$ -CN<sub>pure</sub> solutions increased with increasing concentration at each temperature. However, only at concentrations higher than 0.5% (w/v), visible self-association could be observed for  $\beta$ -CN<sub>conc</sub> samples above 37 °C. This concentration-dependent heat-induced association behaviour of  $\beta$ -CN is in agreement with the findings of previous studies where a minimum concentration of  $\beta$ -CN was required for self-association (Dauphas et al., 2005; O'Connell et al., 2003).

Compared to  $\beta$ -CN<sub>pure</sub> solutions,  $\beta$ -CN<sub>conc</sub> solutions displayed some obvious differences in appearance under the same experimental conditions. For instance, 1%  $\beta$ -CN<sub>conc</sub> was a clear solution at 4°C, whereas  $\beta$ -CN<sub>pure</sub> solution had a very turbid, opaque appearance. These results illustrate that

$\beta$ -CNpure self-associates at lower  $\beta$ -CN concentration than  $\beta$ -CNconc, possibly due to the effect of the other proteins and/or minerals. In further experiments, the thermal aggregation of 0.05%  $\beta$ -CNpure and 1%  $\beta$ -CNconc were studied as they were the most suitable concentrations required to observe the self-assembly of  $\beta$ -CN from a monomeric state to an aggregated state.

### 3.3. Effect of buffer type and $\text{CaCl}_2$ addition on the turbidity and particle size of 0.05% $\beta$ -CNpure solutions

Solution turbidity measurement provided a macroscopic overview of the aggregation of  $\beta$ -CN as influenced by concentration, temperature and choice of ingredient. The size of aggregates is one of the most important factors affecting turbidity of aggregated protein. Changes in turbidity and particle size of 0.05%  $\beta$ -CNpure solutions during a temperature ramp (4 to 55 °C), in different buffers containing  $\text{CaCl}_2$  at varying concentration are presented in Figures 3 and 4, respectively. It is shown that in the absence of added  $\text{CaCl}_2$ , no significant difference in turbidity ( $p > 0.05$ ) was observed at temperatures between 4 and 22 °C, irrespective of buffer type. When the temperature was increased to greater than 25 °C, the turbidity of all  $\beta$ -CNpure solutions increased (Fig. 3A). This turbidity development correlated well with the size measurement (Fig. 4A), which showed that  $\beta$ -CNpure solutions mainly contain particles with volume mean particle size of ~8 nm at low temperatures (4 to 10 °C), indicative of the monomeric form of  $\beta$ -CN (Faizullin, Konnova, Haertlé, & Zuev, 2017; O'Connell et al., 2003). Particle size increased with temperature, most likely due to aggregation.

The addition of 2.5 mM  $\text{CaCl}_2$  caused an increase in particle size of  $\beta$ -CNpure solutions at temperatures from 4 to 16 °C (Fig. 4B). At 4 °C, a mixture of 10 mM  $\text{NaH}_2\text{PO}_4$  buffer and 2.5 mM  $\text{CaCl}_2$  precipitated as calcium phosphate, whereas no precipitation occurred when  $\beta$ -CNpure was present. Crowley (2016) also reported that  $\beta$ -CNconc can prevent calcium phosphate precipitation in simulated milk ultrafiltrate (SMUF) at 37 or 63 °C. It was suggested that ionic calcium induces  $\beta$ -CN aggregation *via* divalent bridges between serine phosphate groups, and thereby preventing calcium phosphate precipitation (Kakalis, Kumosinski, & Farrell, 1990).

At temperatures above 37 °C (Fig. 4B), the particle sizes of both  $\beta$ -CNpure/ $\text{H}_2\text{O}$  and  $\beta$ -CNpure/imidazole solutions with added  $\text{CaCl}_2$  displayed a sharp increase and the sizes were over 1

$\mu\text{m}$  at 50 °C. This was in agreement with the finding by Dauphas et al. (2005) who found large  $\beta\text{-CN}$  aggregates with a diameter of greater than 1  $\mu\text{m}$  at 50 °C and after addition of 10 mM  $\text{CaCl}_2$ . It was suggested that the affinity of  $\beta\text{-CN}$  to  $\text{Ca}^{2+}$  increases with temperature (Horne & Lucey, 2014). However, under the same circumstances, the size of  $\beta\text{-CN}_{\text{pure}}/\text{NaH}_2\text{PO}_4$  solution did not change significantly with the addition of  $\text{CaCl}_2$  (Fig. 4B). The authors assume that a competition between inorganic phosphate and organic phosphoserine groups of  $\beta\text{-CN}$  reacting with  $\text{Ca}^{2+}$  may affect the bridging effect of ionic calcium. The turbidity results of  $\beta\text{-CN}_{\text{pure}}$  solutions with added  $\text{Ca}^{2+}$  showed similar trends in the DLS results (Fig. 3B).

### 3.4. Effect of buffer type and $\text{CaCl}_2$ addition on the turbidity and particle size of 1% $\beta\text{-CN}_{\text{conc}}$ solutions

The turbidity results of 1%  $\beta\text{-CN}_{\text{conc}}$  solutions were in good agreement with the DLS measurement (Fig. 5 and 6). The monomeric form of  $\beta\text{-CN}$  was also detected at 4 °C in the absence of  $\text{CaCl}_2$  (Fig. 6A). Interestingly, heating only caused a slow and slight increase in both size and turbidity in the temperature range 4 to 49 °C, irrespective of buffer type (Fig. 5A and 6A). At temperature greater than 49 °C, a significant increase in turbidity and size for  $\beta\text{-CN}_{\text{conc}}/\text{imidazole}$  and  $\beta\text{-CN}_{\text{conc}}/\text{H}_2\text{O}$  solutions were observed whereas  $\beta\text{-CN}_{\text{conc}}/\text{NaH}_2\text{PO}_4$  solution changed very little with increasing temperature. These results displayed similar trends to those of  $\beta\text{-CN}_{\text{pure}}$  solutions in the presence of  $\text{Ca}^{2+}$  (Fig. 3B and 4B). Calculated Ca and P contents of 0.05%  $\beta\text{-CN}_{\text{pure}}$  solution were 1  $\mu\text{M}$  Ca and 0.1 mM P while 1%  $\beta\text{-CN}_{\text{conc}}$  solution contained 2.5 mM Ca and 2.5 mM P. Therefore in phosphate buffer, 0.05%  $\beta\text{-CN}_{\text{pure}}$  with added 2.5 mM  $\text{Ca}^{2+}$  and 1%  $\beta\text{-CN}_{\text{conc}}$  without added  $\text{Ca}^{2+}$  have a very similar total calcium and phosphate content. Hence they showed very similar aggregation behaviour. Adding 2.5 mM  $\text{CaCl}_2$  to  $\beta\text{-CN}_{\text{conc}}$  solution resulted in a marked increase in both turbidity and size for  $\beta\text{-CN}_{\text{conc}}/\text{imidazole}$  and  $\beta\text{-CN}_{\text{conc}}/\text{H}_2\text{O}$  solutions at all temperatures ( $p < 0.05$ ) (Fig. 5B and 6B). At temperatures greater than 31 °C, the particle size increased significantly with increasing temperature and turbidity remained unchanged at values of 3.5 due to the detection limit of the instrument (Fig. 5B). Visible precipitation was observed for  $\beta\text{-CN}_{\text{conc}}/\text{NaH}_2\text{PO}_4$  solution at 4 °C. It

was assumed that the precipitation is mainly due to the co-precipitated calcium phosphate and casein (Guo, Campbell, Chen, Lenhoff, & Velev, 2003).

### 3.5. Secondary structure of $\beta$ -CN during thermal aggregation

The amide I band in FTIR spectra was used to study changes in the secondary structure of proteins, as it represents a C=O stretch frequencies which is sensitive to its folding environment (Farrell Jr. et al., 2001; Kehoe et al., 2008). Figure 7A showed changes in the amide I region of the FTIR spectra of  $\beta$ -CNpure solution at 0.05% prepared in H<sub>2</sub>O as a function of temperature. The spectra showed that there was little structural change upon heating (4 to 55 °C), with the maximum absorbance shifting from 1660 and 1650 cm<sup>-1</sup>. This is similar to the results of Farrell Jr. et al. (2001) who found a red shift in circular dichroism with temperature.

The subtraction of the sample spectrum at 4 °C from that of samples at  $\geq 16$  °C (Fig. 7B) showed an increase in intensity at 1637 cm<sup>-1</sup> with increasing temperature. This band has been assigned to the intramolecular  $\beta$ -sheet (Tanaka, Morishima, Akagi, Hashikawa, & Nukina, 2001), suggesting an ordered structure in a monomeric state of  $\beta$ -CN (at 4 and 16 °C). It was also noteworthy that aggregation was not *via* inter-molecular  $\beta$ -sheet (expected around 1620 cm<sup>-1</sup>) as observed for most other structured dairy proteins (Kehoe et al., 2008; Lefèvre & Subirade, 2003).

Hence, the question was whether changes in the secondary structure precede aggregation or the other way around. During heating,  $\beta$ -CNpure showed changes in the band around 1637 cm<sup>-1</sup> at temperature as low as 16 °C; changes increased with higher temperatures. However, the particle size in Fig. 5A, at equivalent conditions, only showed changes above 25 °C. This suggests that changes in the secondary structure (increase in intramolecular  $\beta$ -sheets) appeared first, which could induce aggregation of  $\beta$ -CN, rather than the other way around. However, given the small amplitude of changes in the absorption, these conclusions need to be treated with caution. In addition, the above observation could only be made for the higher purity  $\beta$ -CN ( $\beta$ -CNpure) and not for  $\beta$ -CNconc, as discussed.

Very little change in the secondary structure was shown in 1%  $\beta$ -CNcon/H<sub>2</sub>O solution between 4 and 55 °C (Fig. 7), although  $\beta$ -CN self-associated above 49 °C (Fig. 6A). This suggests that the self-

association of  $\beta$ -CN<sub>conc</sub> did not cause any significant conformational change in  $\beta$ -CN, which is also consistent with the results of Farrell Jr. et al. (2001).

It was therefore concluded that the self-association of  $\beta$ -CN had little or no effect on the conformational change of  $\beta$ -CN and vice versa. Addition of 2.5 mM  $\text{CaCl}_2$  to the protein solutions did not alter their spectra for both  $\beta$ -CN<sub>pure</sub> and  $\beta$ -CN<sub>conc</sub> solutions (results not shown).

### 3.6. Microstructure of aggregates

The association and dissociation of  $\beta$ -CN were characterised by light microscopy using a temperature-controlled sample stage.  $\beta$ -CN<sub>pure</sub>/H<sub>2</sub>O,  $\beta$ -CN<sub>pure</sub>/imidazole,  $\beta$ -CN<sub>conc</sub>/H<sub>2</sub>O and  $\beta$ -CN<sub>conc</sub>/imidazole solutions in the presence of  $\text{CaCl}_2$  were selected for microscopy analysis because the particle size measurement showed that they were large enough ( $> 500$  nm) at high temperatures for visualisation. Visible aggregates appeared at 37 °C after 20 min in 1%  $\beta$ -CN<sub>conc</sub> solutions, which confirms that self-association had occurred. However, no particles were observed by light microscopy in 0.05%  $\beta$ -CN<sub>pure</sub> solutions after incubated at 55 °C for 4 h due to the low protein concentration. Therefore, 1%  $\beta$ -CN<sub>pure</sub> solutions were used to monitor the microstructure of  $\beta$ -CN<sub>pure</sub> aggregates. Figure 8 (A-H) showed DIC images of temperature-dependent 1%  $\beta$ -CN<sub>pure</sub>/imidazole solution as a function of temperature and time in the presence of 2.5 mM  $\text{CaCl}_2$ . No particles were visualized at temperatures of 10, 25 and 37 °C (Fig. 8A, B and C), due to the limitation of the microscope resolution. Aggregates were observed at 55 °C after 20 min (Fig. 8D) and the particles look spherical and seem to be uniform in size, which indicates that self-association had taken place. When the sample was heated at 55 °C for up to 4 h, particle size increased ( $> 1$   $\mu\text{m}$ ), with a rounded shape (Fig. 8E).

Interestingly, the shape of  $\beta$ -CN<sub>pure</sub> aggregates changed when the sample was cooled down to 37 °C (Fig. 8E and F). In previous studies,  $\beta$ -CN aggregates changed from an oblate ellipsoid to spheroid with temperature was reported by Kajiwaru et al. (1988). Small and oblate micelles (Portnaya et al., 2006) or flat disk-like micelles (Moitzi, Portnaya, Glatter, Ramon, & Danino, 2008) have also been observed using cryogenic transmission electron microscopy. In Figure 8G, temperature was cooled to 25 °C, very few  $\beta$ -CN aggregates were visible (Fig. 8G). They completely disappeared at 10 °C after



20 min (Fig. 8H), suggesting that thermal aggregation of  $\beta$ -CN for the select samples is reversible but that the rate of dissociation is slower than that of association although the heating and cooling rate are the same.

Compared with 1%  $\beta$ -CN<sub>pure</sub>\_imidazole solution, 1%  $\beta$ -CN<sub>conc</sub>\_imidazole solution with 2.5 mM  $\text{CaCl}_2$  showed very similar self-association and dissociation behaviour during heating followed by cooling (Fig. 9A-H). However, it was found that 1%  $\beta$ -CN<sub>conc</sub>\_imidazole solution formed larger aggregates than  $\beta$ -CN<sub>pure</sub> under the same conditions (Fig. 9C-F). Increasing heating time led to an increase in particle size and a few irregularly shaped aggregates were produced (Fig. 9E, white arrow). Slight changes in shape during heating or cooling were probably due to the association or dissociation of  $\beta$ -CN.

#### 4. Conclusion

This study demonstrates that both  $\beta$ -CN products showed self-association at elevated temperature. Different aggregation behaviours were observed, depending on  $\beta$ -CN purity, protein concentration, buffer type and  $\text{CaCl}_2$  addition. Generally, adding  $\text{CaCl}_2$  promoted thermal aggregation of  $\beta$ -CN and led to larger aggregates ( $> 500$  nm), which were visible using light microscopy. However, in the presence of a certain amount of phosphate and calcium ( $\text{Ca:P} \sim 1:4$  in this study), the aggregation was inhibited even at high temperatures ( $55^\circ\text{C}$ ). The new findings of this work are of relevance to end-users of  $\beta$ -casein enriched ingredients in controlling aggregation of  $\beta$ -CN by changing the ratio of calcium:phosphate, temperature and selected ingredients, to optimise the quality and functionality of  $\beta$ -CN-enriched dairy products.

## 5. Acknowledgements

This work was funded by the Irish Dairy Levy Research Trust (project number MDDT 6261). Ms. Li was funded under the Teagasc Walsh Fellowship Scheme. The authors would like to acknowledge Prof. John Lucey and Mr. Mike Molitor (Center for Dairy Research and University of Wisconsin-Madison, Madison, USA) for their kind donation of the  $\beta$ -CN concentrate powder used in this study.

## 6. References

- Andrews, A. L., Atkinson, D., Evans, M. T. A., Finer, E. G., Green, J. P., Phillips, M. C., & Robertson, R. N. (1979). The conformation and aggregation of bovine  $\beta$ -casein A. I. Molecular aspects of thermal aggregation. *Biopolymers*, 18(5), 1105-1121.
- Atamer, Z., Post, A. E., Schubert, T., Holder, A., Boom, R. M., & Hinrichs, J. (2017). Bovine  $\beta$ -casein: Isolation, properties and functionality. A review. *International Dairy Journal*, 66, 115-125.
- Crowley, S. V. (2016). *Physicochemical characterisation of protein ingredients prepared from milk by ultrafiltration or microfiltration for application in formulated nutritional products*. PhD thesis, University College Cork, Cork, Ireland. Available online: <https://cora.ucc.ie/handle/10468/3243?show=full>.
- Darewicz, M., Dziuba, J., Caessens, P. W. J. R., & Gruppen, H. (2000). Dephosphorylation-induced structural changes in  $\beta$ -casein and its amphiphilic fragment in relation to emulsion properties. *Biochimie*, 82(3), 191-195.
- Dauphas, S., Mouhous-Riou, N., Metro, B., Mackie, A. R., Wilde, P. J., Anton, M., & Riaublanc, A. (2005). The supramolecular organisation of  $\beta$ -casein: effect on interfacial properties. *Food Hydrocolloids*, 19(3), 387-393.
- de Kruif, C. G., & Grinberg, V. Y. (2002). Micellisation of  $\beta$ -casein. *Colloids and Surfaces A: Physicochemical and Engineering Aspects*, 210(2-3), 183-190.
- Dickinson, E. (2001). Milk protein interfacial layers and the relationship to emulsion stability and rheology. *Colloids and Surfaces B: Biointerfaces*, 20(3), 197-210.
- Dickinson, E., Rolfe, S. E., & Dalgleish, D. G. (1988). Competitive adsorption of  $\alpha$ s1-casein and  $\beta$ -casein in oil-in-water emulsions. *Food Hydrocolloids*, 2(5), 397-405.
- Evans, M. T. A., Phillips, M. C., & Jones, M. N. (1979). The conformation and aggregation of bovine  $\beta$ -casein A. II. Thermodynamics of thermal association and the effects of changes in polar and apolar interactions on micellization. *Biopolymers*, 18(5), 1123-1140.
- Faizullin, D. A., Konnova, T. A., Haertlé, T., & Zuev, Y. F. (2017). Secondary structure and colloidal stability of beta-casein in microheterogeneous water-ethanol solutions. *Food Hydrocolloids*, 63(Supplement C), 349-355.
- Farrell Jr., H. M. (1999). Milk synthesis and composition. In E. Knobil & J. D. Neill (Eds.), *Encyclopedia of Reproduction* (Vol. 3, pp. 256-263). New York: Academic Press
- Farrell Jr., H. M., Wickham, E. D., Unruh, J. J., Qi, P. X., & Hoagland, P. D. (2001). Secondary structural studies of bovine caseins: temperature dependence of  $\beta$ -casein structure as analyzed by circular dichroism and FTIR spectroscopy and correlation with micellization. *Food Hydrocolloids*, 15(4-6), 341-354.
- Fox, P. F., & McSweeney, P. L. H. (2003). *Advanced Dairy Chemistry: Volume 1: Proteins, Parts A&B* (3rd ed. Vol. 1). New York: Kluwer Academic/Plenum Publishers.
- Greenberg, R., Groves, M. L., & Dower, H. J. (1984). Human beta-casein. Amino acid sequence and identification of phosphorylation sites. *Journal of Biological Chemistry*, 259, 5132-5138.
- Guo, C., Campbell, B. E., Chen, K., Lenhoff, A. M., & Velev, O. D. (2003). Casein precipitation equilibria in the presence of calcium ions and phosphates. *Colloids and Surfaces B: Biointerfaces*, 29(4), 297-307.
- Holt, C., & Sawyer, L. (1993). Caseins as rheomorphic proteins: interpretation of primary and secondary structures of the  $\alpha$ s1-,  $\beta$ - and  $\kappa$ -caseins. *Journal of the Chemical Society, Faraday Transactions*, 89(15), 2683-2692.
- Horne, D. S. (1998). Casein Interactions: Casting Light on the Black Boxes, the Structure in Dairy Products. *International Dairy Journal*, 8(3), 171-177.
- Horne, D. S., & Lucey, J. A. (2014). Revisiting the temperature dependence of the coagulation of renneted bovine casein micelles. *Food Hydrocolloids*, 42, 75-80.
- Huppertz, T. (2013). Chemistry of the Caseins. In P. L. H. M. P. F. Fox (Ed.), *Advanced Dairy Chemistry Volume 1A: Proteins: Basic Aspects* (4 ed., pp. 135-155). New York: Springer.

- Huppertz, T., Hennebel, J.-B., Considine, T., Shakeel Ur, R., Kelly, A. L., & Fox, P. F. (2006). A method for the large-scale isolation of  $\beta$ -casein. *Food Chemistry*, 99(1), 45-50.
- Kajiwara, K., Niki, R., Urakawa, H., Hiragi, Y., Donkai, N., & Nagura, M. (1988). Micellar structure of  $\beta$ -casein observed by small-angle X-ray scattering. *Biochimica et Biophysica Acta (BBA) - Protein Structure and Molecular Enzymology*, 955(2), 128-134.
- Kakalis, L. T., Kumosinski, T. F., & Farrell, H. M. (1990). A multinuclear, high-resolution NMR study of bovine casein micelles and submicelles. *Biophysical Chemistry*, 38(1), 87-98.
- Kehoe, J. J., Remondetto, G. E., Subirade, M., Morris, E. R., & Brodkorb, A. (2008). Tryptophan-mediated denaturation of  $\beta$ -lactoglobulin A by UV irradiation. *Journal of Agricultural and Food Chemistry*, 56(12), 4720-4725.
- Lefèvre, T., & Subirade, M. (2003). Formation of intermolecular  $\beta$ -sheet structures: a phenomenon relevant to protein film structure at oil-water interfaces of emulsions. *Journal of Colloid and Interface Science*, 263(1), 59-67.
- Li, M., Auty, M. A. E., O'Mahony, J. A., Kelly, A. L., & Brodkorb, A. (2016). Covalent labelling of  $\beta$ -casein and its effect on the microstructure and physico-chemical properties of emulsions stabilized by  $\beta$ -casein and whey protein isolate. *Food Hydrocolloids*, 61, 504-513.
- McCarthy, N. A., Kelly, A. L., O'Mahony, J. A., & Fenelon, M. A. (2013). The physical characteristics and emulsification properties of partially dephosphorylated bovine  $\beta$ -casein. *Food Chemistry*, 138(2-3), 1304-1311.
- McSweeney, S., O'Regan, J., & O'Callaghan, D. (2013). Nutritional formulae for infants and young children. In Y. W. P. G. F. W. Haenlein (Ed.), *Milk and Dairy Products in Human Nutrition: Production, Composition and Health* (1 ed., pp. 462). UK: John Wiley & Sons.
- Meisel, H. (1997). Biochemical properties of regulatory peptides derived from mil proteins. *Peptide Science*, 43(2), 119-128.
- Mikheeva, L. M., Grinberg, N. V., Grinberg, V. Y., Khokhlov, A. R., & de Kruif, C. G. (2003). Thermodynamics of micellization of bovine  $\beta$ -casein studied by high-sensitivity differential scanning calorimetry. *Langmuir*, 19(7), 2913-2921.
- Moitzi, C., Portnaya, I., Glatter, O., Ramon, O., & Danino, D. (2008). Effect of Temperature on Self-Assembly of Bovine  $\beta$ -Casein above and below Isoelectric pH. Structural Analysis by Cryogenic-Transmission Electron Microscopy and Small-Angle X-ray Scattering. *Langmuir*, 24(7), 3020-3029.
- Noelken, M., & Reibstein, M. (1968). Conformation of  $\beta$ -casein B. *Archives of Biochemistry and Biophysics*, 123(2), 397-402.
- O'Connell, J. E., Grinberg, V. Y., & de Kruif, C. G. (2003). Association behavior of  $\beta$ -casein. *Journal of Colloid and Interface Science*, 258(1), 33-39.
- O'Mahony, J., Smith, K., & Lucey, J. (2014). Purification of beta casein from milk. In US.
- Ossowski, S., Jackson, A., Obiols-Rabasa, M., Holt, C., Lenton, S., Porcar, L., Paulsson, M., & Nylander, T. (2012). Aggregation behavior of bovine  $\kappa$ - and  $\beta$ -casein studied with small angle neutron scattering, light scattering, and cryogenic transmission electron microscopy. *Langmuir*, 28(38), 13577-13589.
- Panouillé, M., Durand, D., & Nicolai, T. (2005). Jamming and gelation of dense  $\beta$ -Casein micelle suspensions. *Biomacromolecules*, 6(6), 3107-3111.
- Parkinson, E. L., & Dickinson, E. (2004). Inhibition of heat-induced aggregation of a  $\beta$ -lactoglobulin-stabilized emulsion by very small additions of casein. *Colloids and Surfaces B: Biointerfaces*, 39(1-2), 23-30.
- Portnaya, I., Cogan, U., Livney, Y. D., Ramon, O., Shimoni, K., Rosenberg, M., & Danino, D. (2006). Micellization of bovine  $\beta$ -casein studied by isothermal titration microcalorimetry and cryogenic transmission electron microscopy. *Journal of Agricultural and Food Chemistry*, 54(15), 5555-5561.
- Qi, P. X., Wickham, E. D., & Farrell, H. M. (2004). Thermal and alkaline denaturation of bovine  $\beta$ -casein. *The Protein Journal*, 23(6), 389-402.

- 472 Rollema, H. S. (1992). Casein association and micelle formation. In P. F. FOX (Ed.), *Advanced Dairy*  
473 *Chemistry: Proteins* (Vol. 1, pp. 111-141). London: Elsevier Science Publishers.
- 474 Tanaka, M., Morishima, I., Akagi, T., Hashikawa, T., & Nukina, N. (2001). Intra- and intermolecular  $\beta$ -  
475 pleated sheet formation in glutamine-repeat inserted myoglobin as a model for  
476 polyglutamine diseases. *Journal of Biological Chemistry*, 276(48), 45470-45475.
- 477 Yong, Y. H., & Foegeding, E. A. (2008). Effects of caseins on thermal stability of bovine  $\beta$ -lactoglobulin.  
478 *Journal of Agricultural and Food Chemistry*, 56(21), 10352-10358.

479

Figure 1. Reversed-phase high-performance liquid chromatography profiles of proteins in (A)  $\beta$ -CNpure and (B)  $\beta$ -CNconc; (C) Reducing SDS-PAGE of skim milk as a standard (lane 1),  $\beta$ -CNpure (0.05%, w/v of total protein, lane 2), and  $\beta$ -CNconc (0.05%, w/v of total protein, lane 3); Lane M shows the molecular weight markers.

Figure 2. Visual appearance of  $\beta$ -CNpure and  $\beta$ -CNconc in 10 mM sodium phosphate buffer, pH 6.8 at different  $\beta$ -CN concentrations (0.05%-1%) and temperatures (4, 37 and 55 °C).

Figure 3. Temperature-dependent changes in turbidity of 0.05%  $\beta$ -CNpure solutions in the absence (A) or presence of 2.5 mM  $\text{CaCl}_2$  (B), at pH 6.8 in different diluting buffers: water ( $\circ$ ), 10 mM sodium phosphate buffer (X) and 10 mM imidazole buffer ( $\Delta$ ). Error bars indicate standard deviations ( $n \geq 3$ ).

Figure 4. Temperature-dependent changes in the z-average particle size of 0.05%  $\beta$ -CNpure solutions in the absence (A) or presence of 2.5 mM  $\text{CaCl}_2$  (B), at pH 6.8 in different diluting buffers: water ( $\circ$ ), 10 mM sodium phosphate buffer (X) and 10 mM imidazole buffer ( $\Delta$ ).

Figure 5. Temperature-dependent changes in turbidity of 1%  $\beta$ -CNconc solutions in the absence (A) or presence of 2.5 mM  $\text{CaCl}_2$  (B), at pH 6.8 in different diluting buffers: water ( $\circ$ ), 10 mM sodium phosphate buffer (X) and 10 mM imidazole buffer ( $\Delta$ ). Error bars indicate standard deviations ( $n \geq 3$ ).

Figure 6. Temperature-dependent changes in the z-average particle size of 1%  $\beta$ -CNconc solutions in the absence (A) or presence of 2.5 mM  $\text{CaCl}_2$  (B), at pH 6.8 in different diluting buffers: water ( $\circ$ ), 10 mM sodium phosphate buffer (X) and 10 mM imidazole buffer ( $\Delta$ ).

Figure 7. FTIR spectra: vector-normalized amide I bands of 0.05%  $\beta$ -CNpure (A) in water at increasing temperatures from 4 to 55 °C and FTIR spectra with the spectrum of the sample at 4 °C subtracted (B); and vector-normalized amide I bands of 1%  $\beta$ -CNconc (C) in water at increasing temperatures from 4 to 55 °C and FTIR spectra with the spectrum of the sample at 4 °C subtracted (D). The arrow and dashed line indicate an increase in intensity at  $1637\text{ cm}^{-1}$  with increasing temperature.

Figure 8. Micrographs of 1%  $\beta$ -CNpure solution in presence of 2.5 mM  $\text{CaCl}_2$  during heating (10 to 55 °C, top row panel A to D), followed by cooling (55 to 10 °C, bottom row panel E to H) obtained by light microscope in DIC mode. The black line represents the temperature vs. time curve for the whole measurement. Black arrows indicate the time point at which the images were taken. Before cooling, sample was incubated at 55 °C for 4 h. (F) inset shows oblate spheroid shaped  $\beta$ -CN aggregates. Scale bar: 20  $\mu\text{m}$ .

Figure 9. Micrographs of 1%  $\beta$ -CNconc solution in presence of 2.5 mM  $\text{CaCl}_2$  during heating (10 to 55 °C, top row panel A to D), followed by cooling (55 to 10 °C, bottom row panel E to H) obtained by light microscope in DIC mode. The black line represents the temperature vs. time curve for the whole measurement. Black arrows indicate the time point at which the images were taken. Before cooling, sample was incubated at 55 °C for 4 h. (E) inset shows non-spherical shaped aggregates. Scale bar: 20  $\mu\text{m}$ .



Table 1. Compositional data of  $\beta$ -CN ingredients

	$\beta$ -CNpure*	$\beta$ -CNconc
Protein content (% , w/w of powder)	85	87.1
Protein purity ** (% , w/w of total protein)		
Total casein	96.6	83.9
$\alpha$ -casein	1.1	1.2
$\beta$ -casein	90	80
$\kappa$ -casein	5.5	2.7
Total whey protein	3.4	16.1
$\alpha$ -lactalbumin	-	1.4
$\beta$ -lactoglobulin	3.4	14.7
Mineral profile *** (mg/100g)		
Na	132.8 $\pm$ 1.0	92.3 $\pm$ 3.8
Mg	0.90 $\pm$ 0.02	98 $\pm$ 6
P	524 $\pm$ 0.5	531.3 $\pm$ 16.9
K	10.6 $\pm$ 0.1	415 $\pm$ 17
Ca	8.1 $\pm$ 0.6	688 $\pm$ 20

\*One lot of commercial  $\beta$ -CNpure (lot SLBS9719, C6905, Sigma-Aldrich) was used for protein and mineral analysis

\*\*Individual proteins were characterised by RP-HPLC.

\*\*\*Mineral content was measured by ICP-MS method.

Figure 1

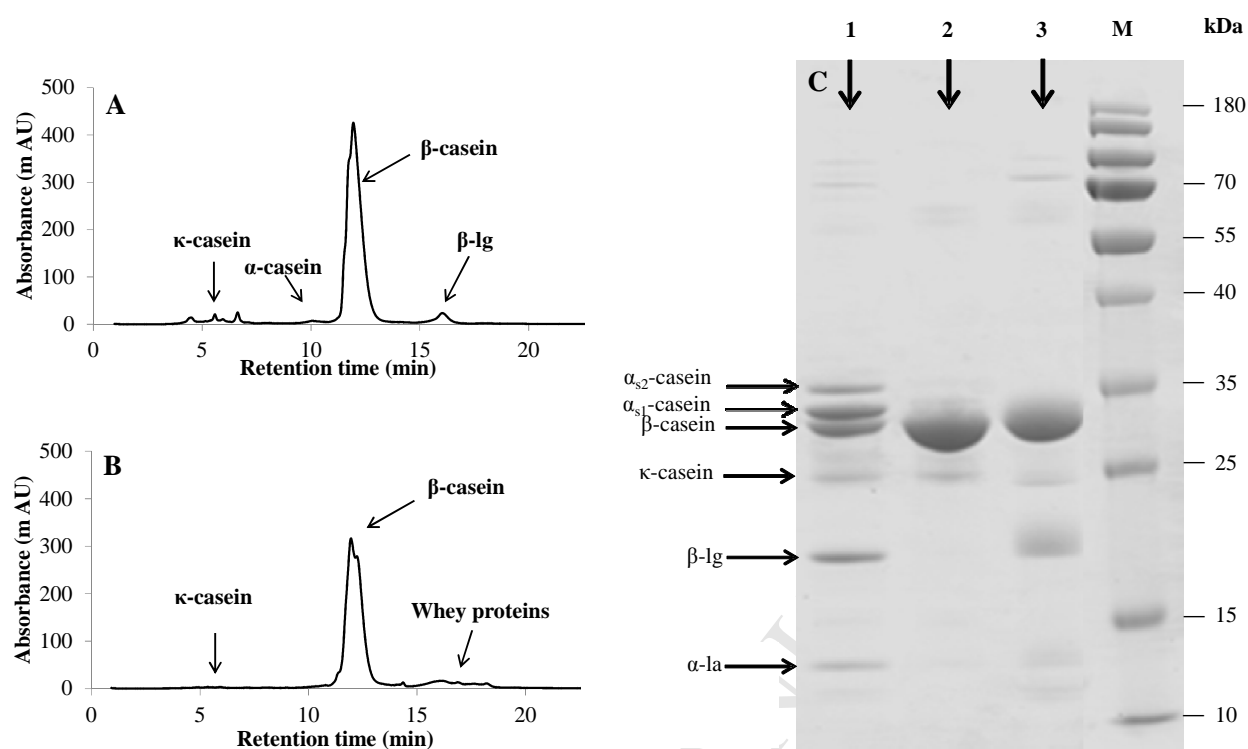


Figure 2

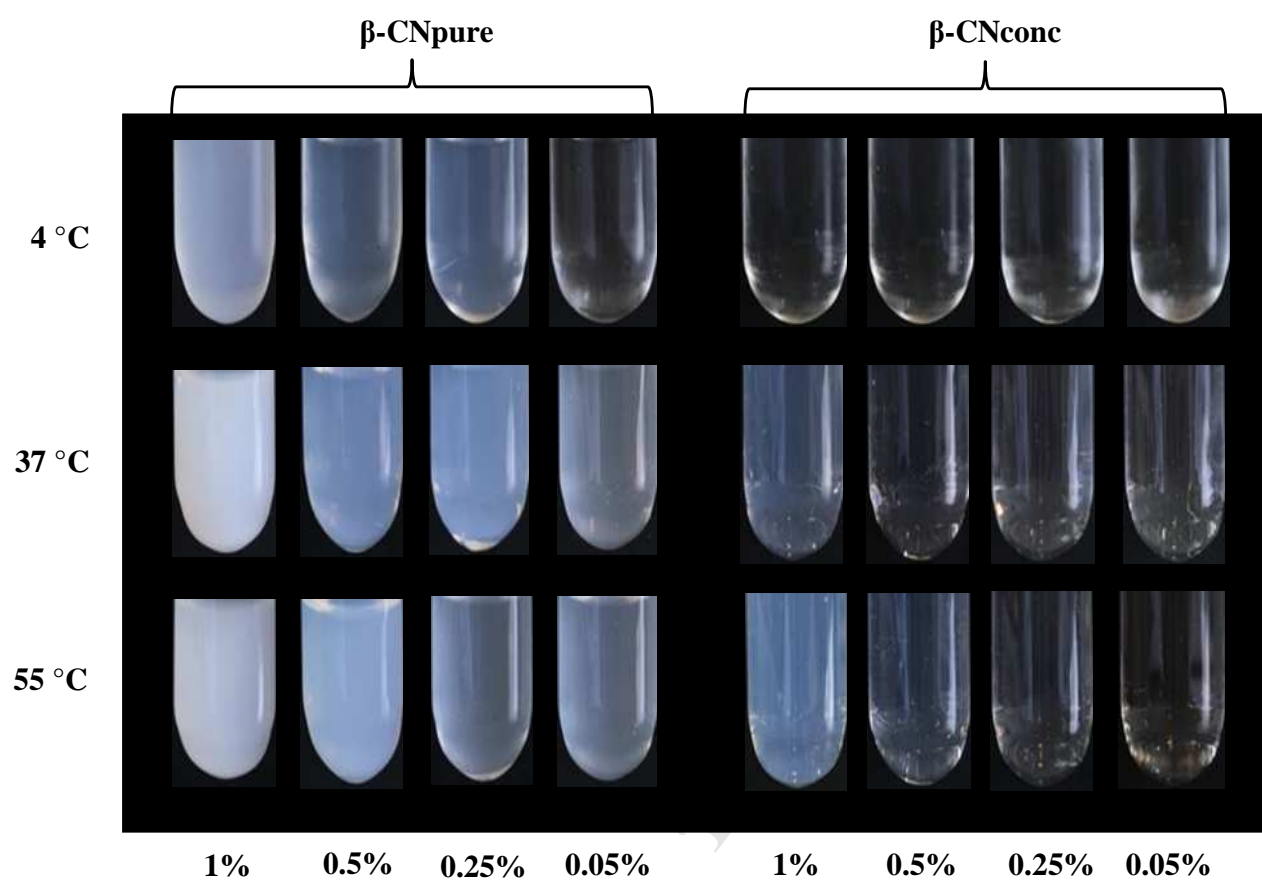


Figure 3

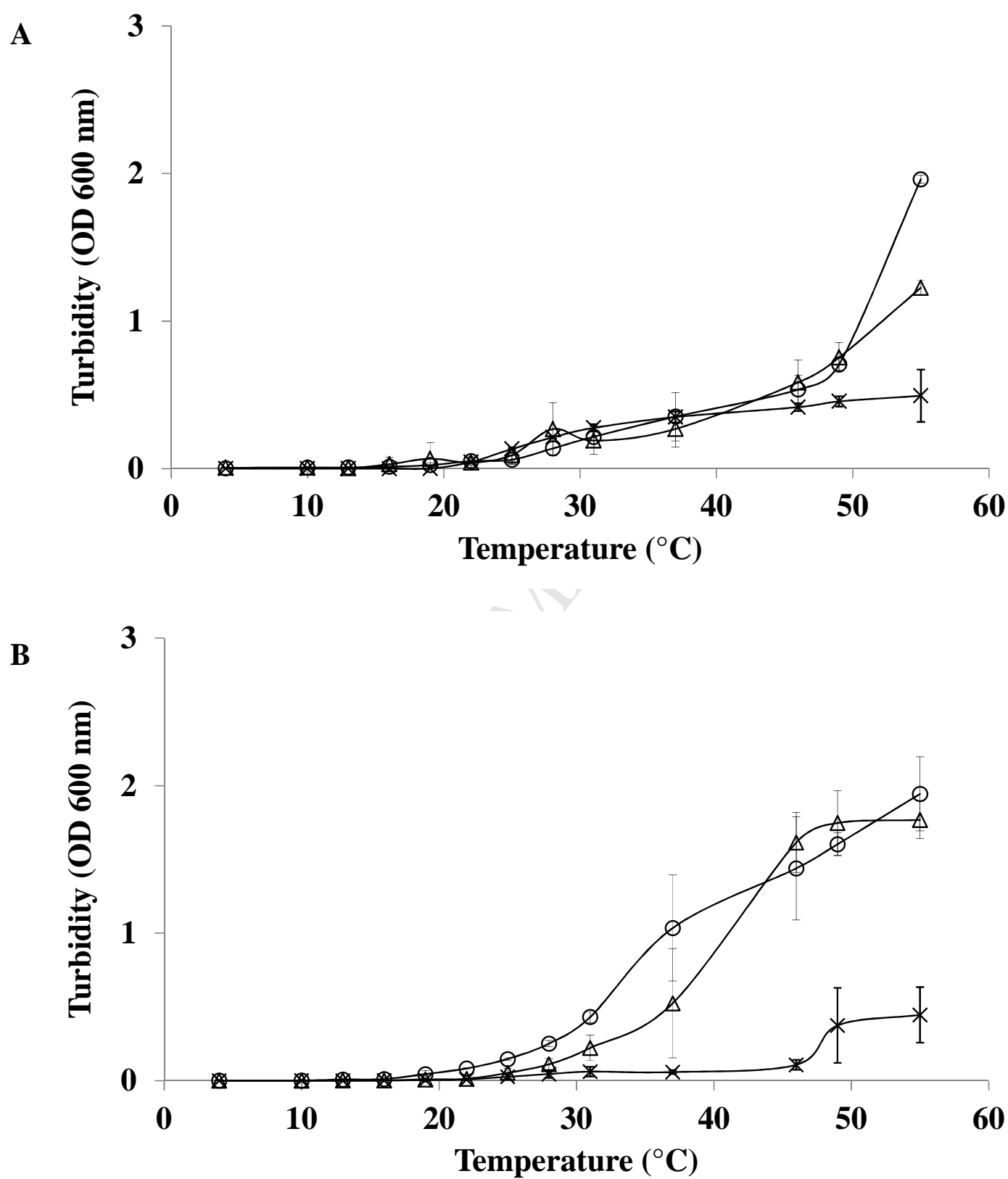


Figure 4

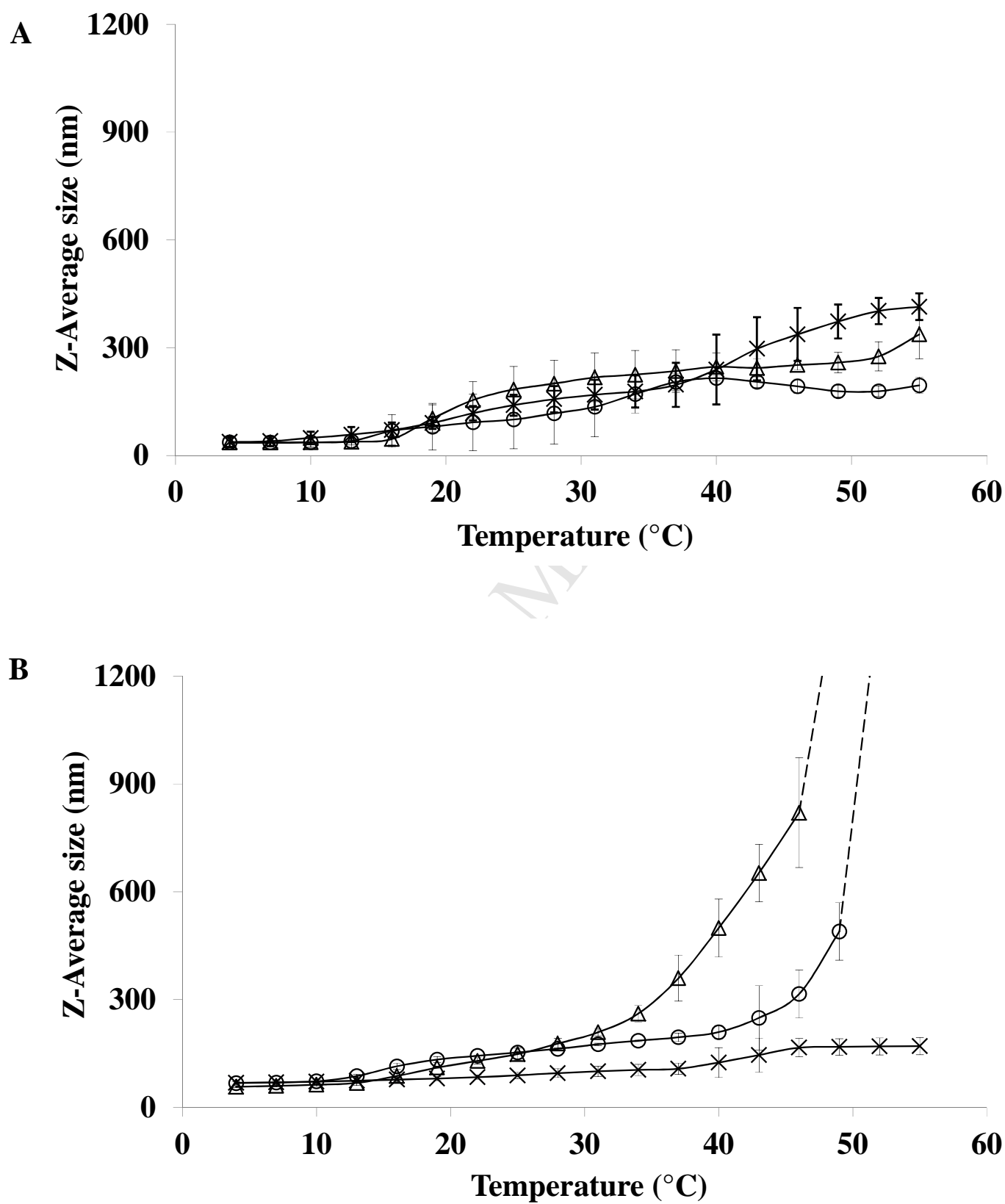


Figure 5

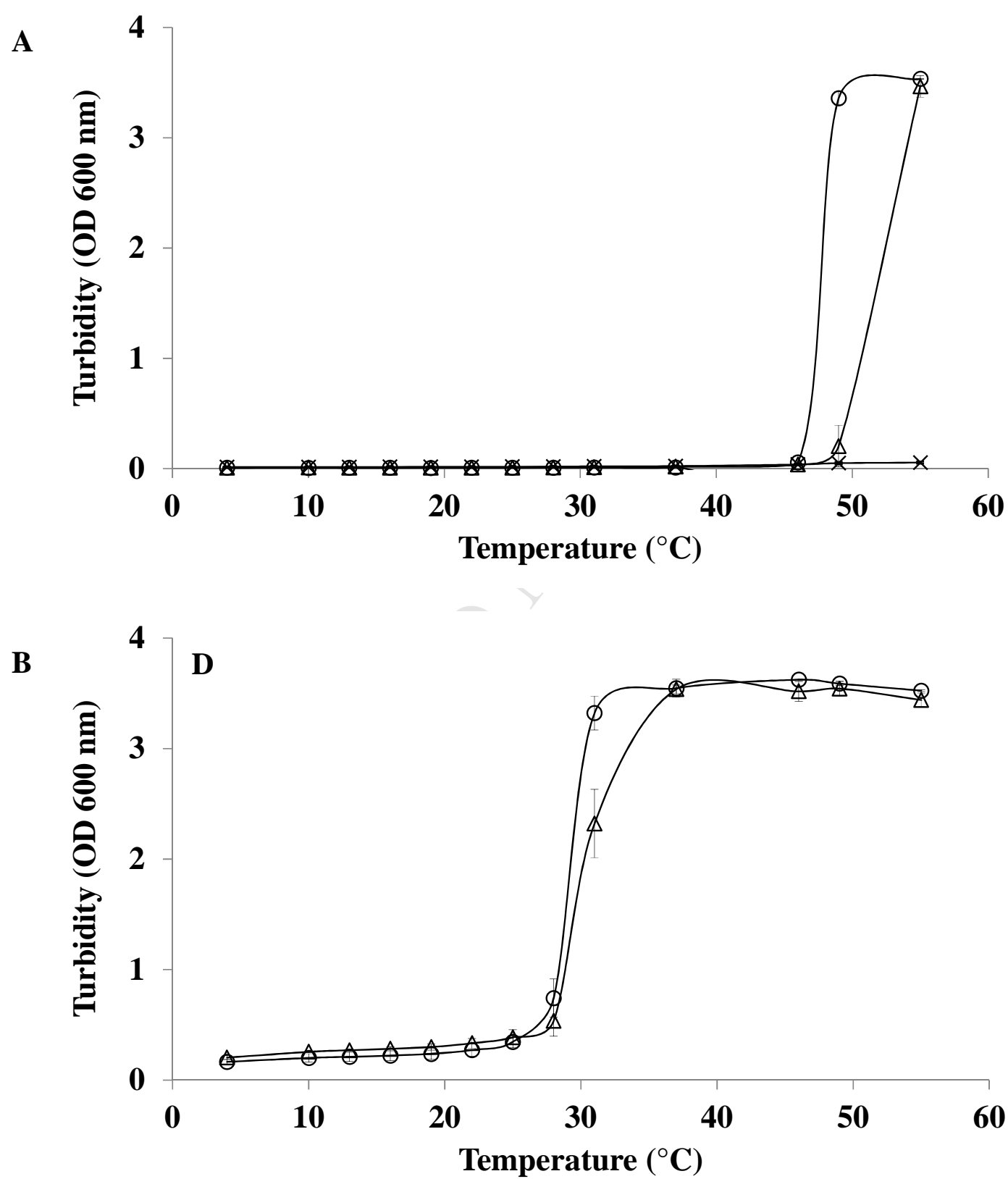


Figure 6

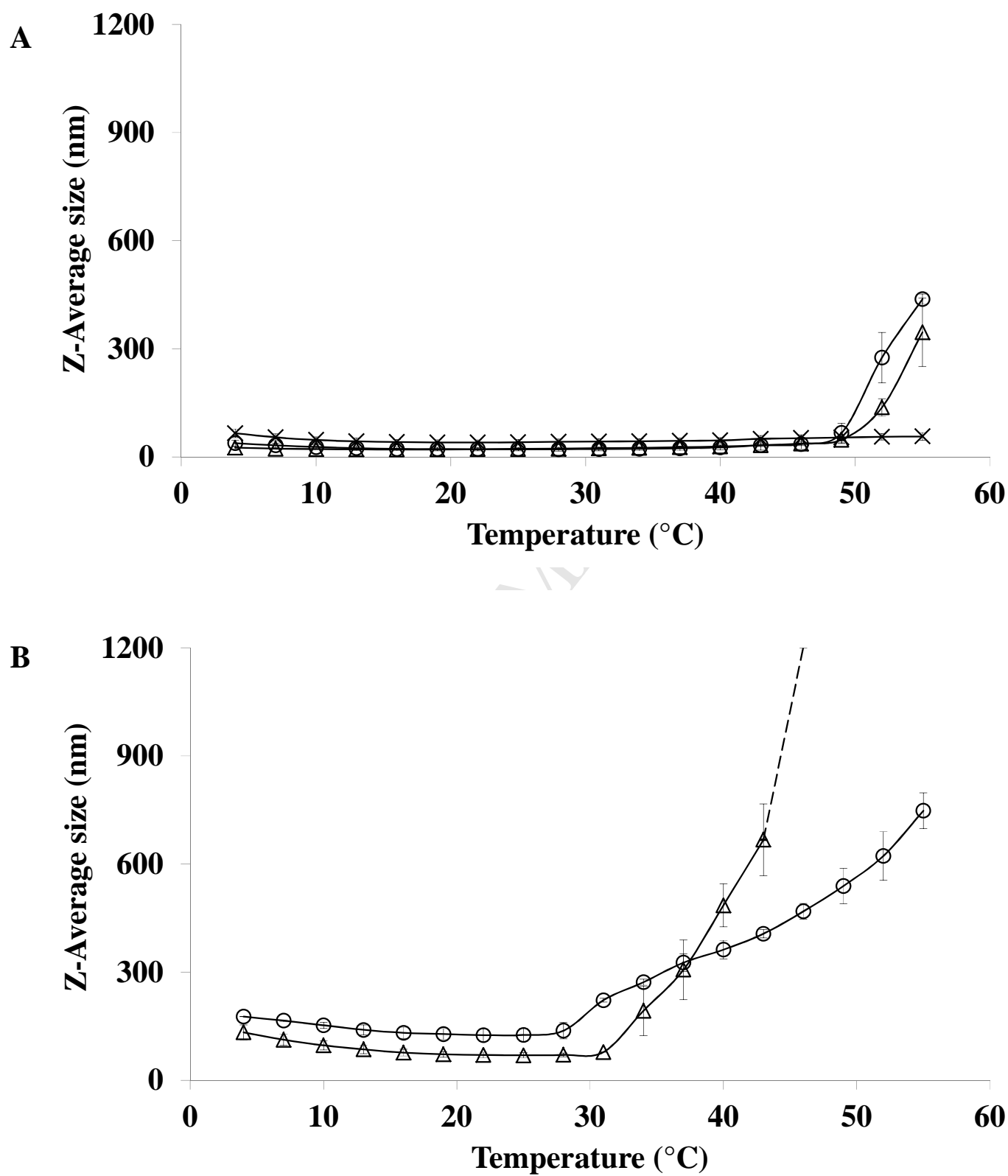
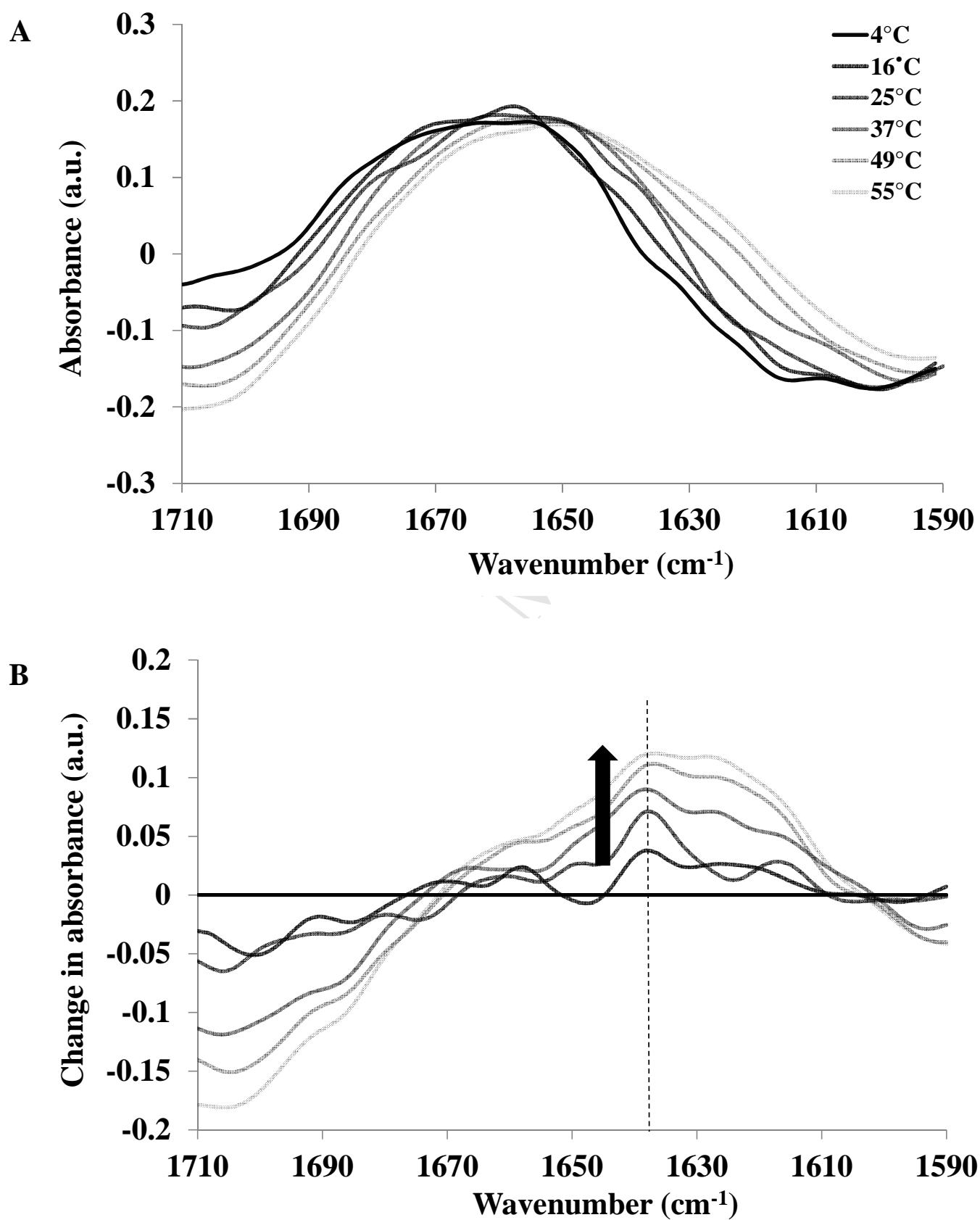


Figure 7





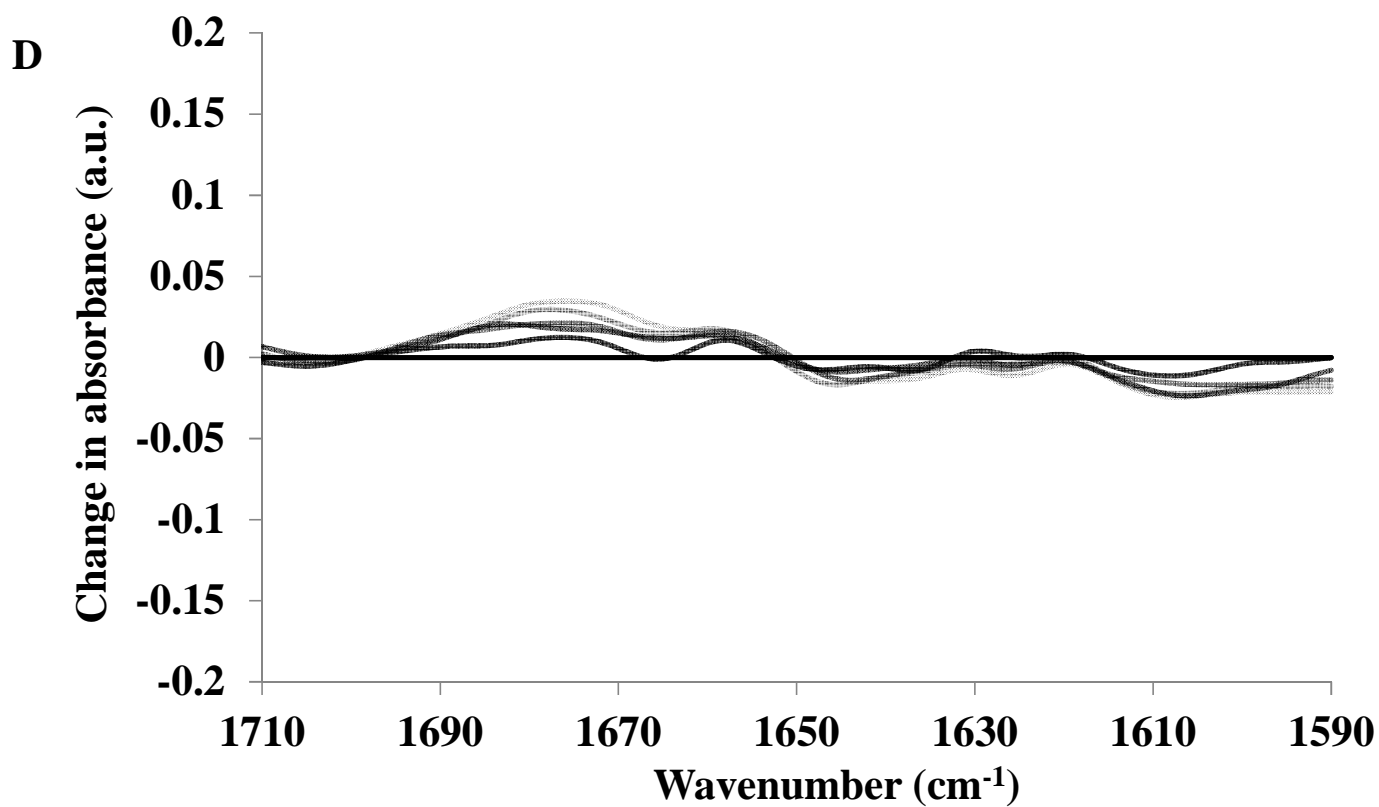
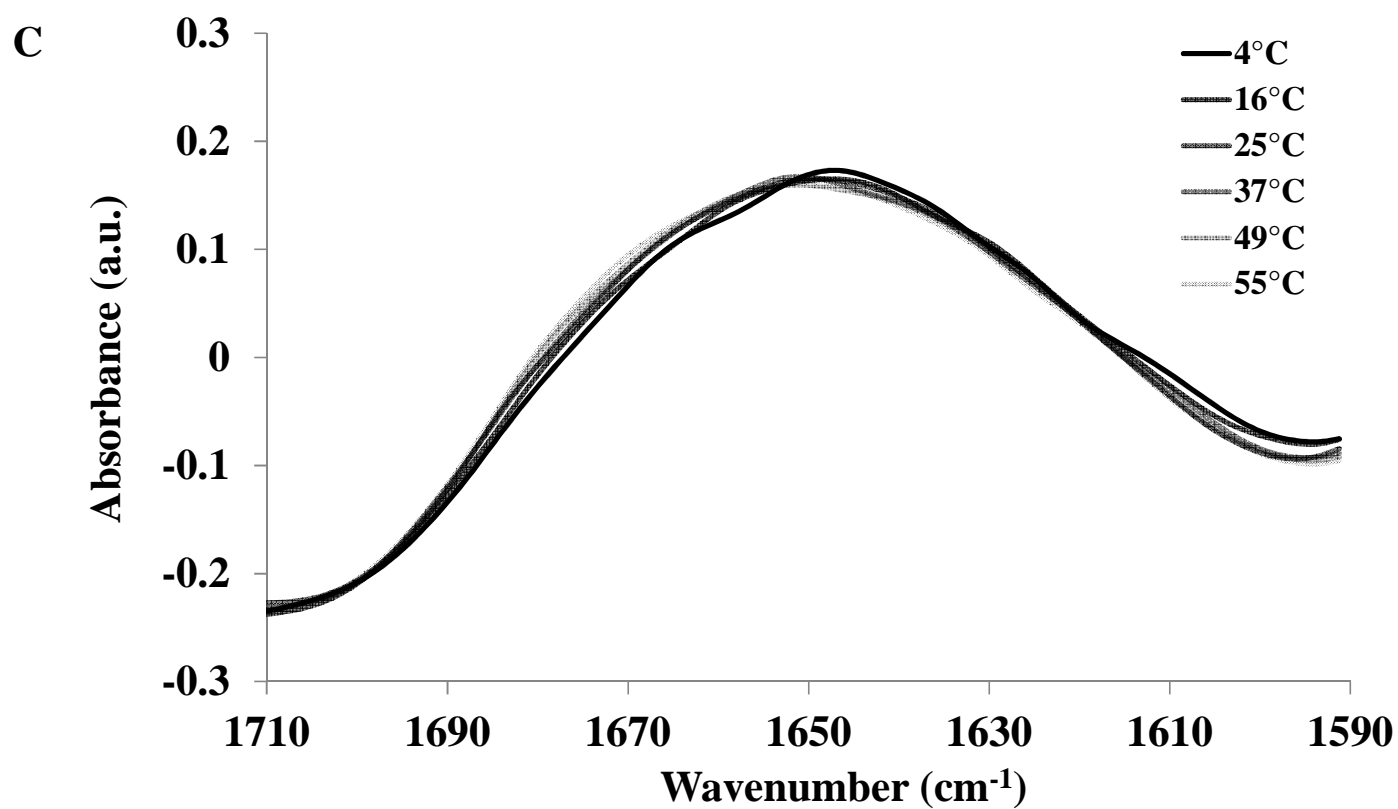


Figure 8

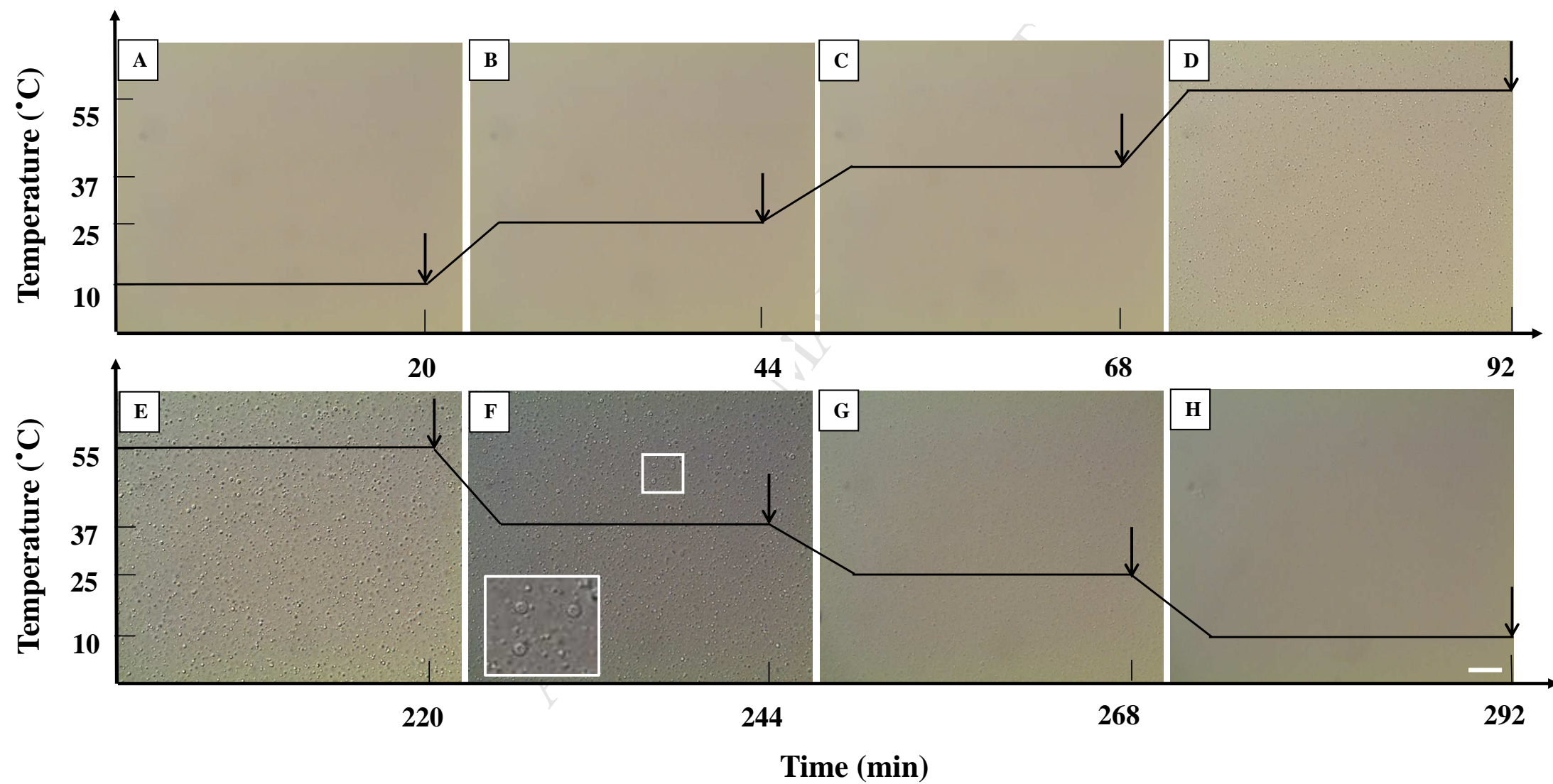
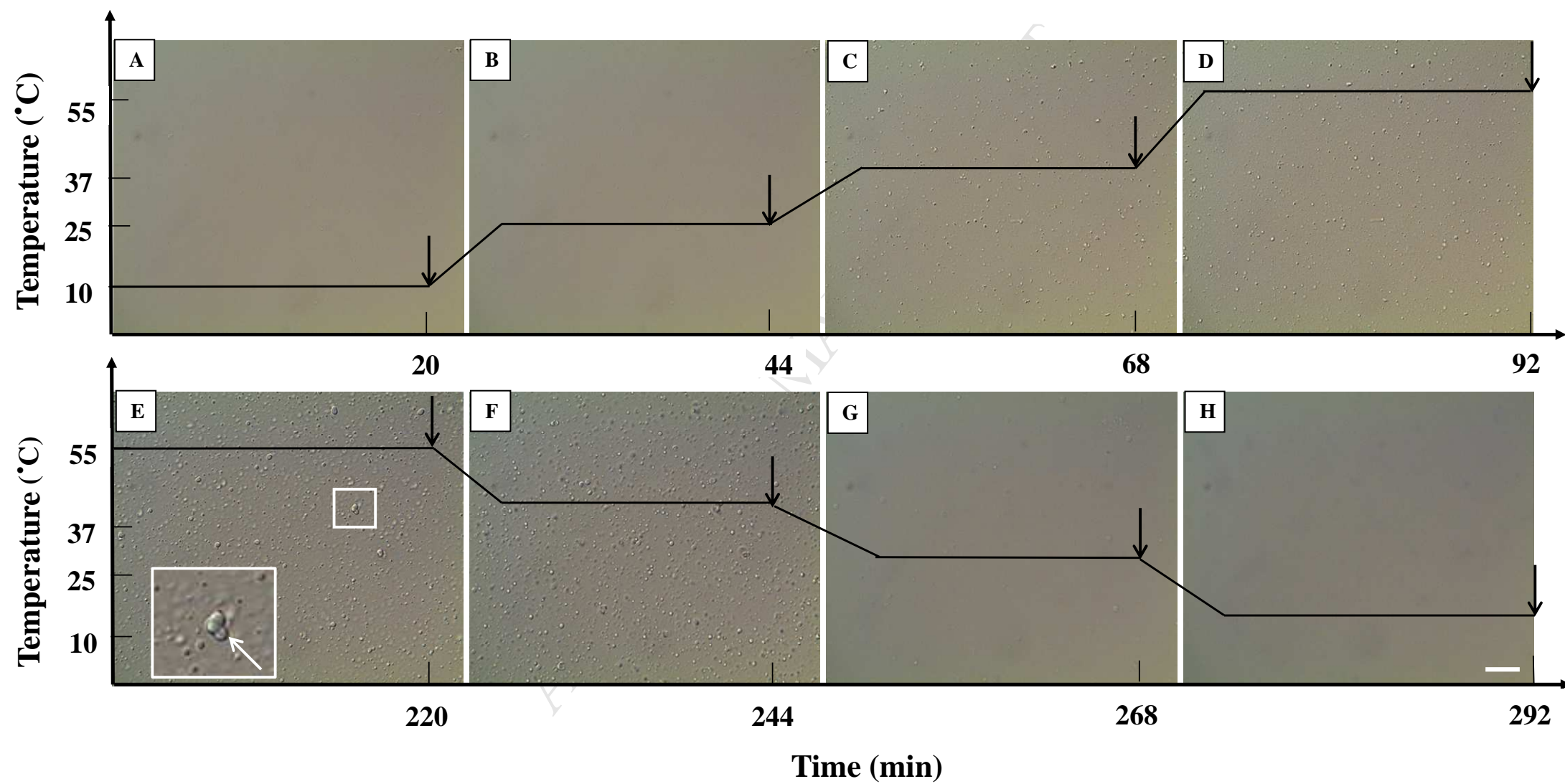


Figure 9



ACCEPTED MANUSCRIPT

## Highlights

- Self-association of  $\beta$ -casein was observed upon heating
- Self-association was strongly dependent on the purity of the protein
- Calcium addition induced the aggregation of  $\beta$ -casein in water and imidazole buffer but not in sodium phosphate buffer.
- Thermo-reversible, spherical and heterogeneous  $\beta$ -casein aggregates were observed at temperatures above 37 °C using light microscopy.